Transient Characteristics of a Single-Effect Absorption Refrigeration Cycle

■

A. Iranmanesh[1], M.A. Mehrabian[2*]

■

[1] Department of Mechanical Engineering (MSc student), Shahid Bahonar University of Kerman, Kerman, I.R. Iran
iranmanesh.aghil@gmail.com

[2] Department of Mechanical Engineering (Professor), Shahid Bahonar University of Kerman, Kerman, I.R. Iran
ma_mehrabian@uk.ac.ir

■

■

Abstract

This paper deals with a lumped-parameter dynamic simulation of a single-effect LiBr-H_2O absorption chiller. In many studies the thermodynamic properties of LiBr-H_2O solution were taken from some approximate relations causing the results to be somewhat inaccurate. These relations were used to solve simultaneous differential equations involving the continuity of species constituting the LiBr-H_2O solution, momentum equations, and energy balances. To diminish the effect of these approximate relations on the results, in this study the thermodynamic properties were taken from the EES software. By making a link between EES and MATLAB softwares, the simultaneous differential equations were solved in MATLAB environment and this process was continued until the convergence criterion was satisfied. Moreover, this study considers the effect of quality on the concentration of solution at the exits of generator and absorber. This effect was ignored in the previous works. In other words, the concentrations of solution at the generator and absorber were not assumed to be equal to the corresponding concentration at the exit of those components in this model. Furthermore, a transient analysis of exergy is accomplished. As time passes, both the coefficient of performance and exergetic efficiency decrease, approaching the steady-state values. The results deduced from the dynamic simulation are compared with those in steady-state condition. The comparison shows that the transient simulation predictions are in close agreement with steady-state results.

Keywords: Absorption chillers, LiBr-H_2O, Single-effect, Transient behavior.

---

* **Corresponding Author**

1. Introduction

Nowadays, researchers are prompted to reconsider the absorption refrigeration systems because of the increasing anxiety on the depletion of ozone layer and global warming. Absorption systems use the working fluids not dangerous to the environment and the input energy to the absorption chiller is heat, rather than mechanical work. Different heat sources can be applied in the absorption chillers such as solar and geothermal energy, as well as waste heat released from industrial machines.

Many studies were conducted on the steady-state and dynamic simulation of absorption chillers so far. Jeong, et al. [1] developed a numerical model for the dynamic simulation of a steam-driven LiBr-H$_2$O absorption heat pump for recovering low-grade waste heat. Storage terms with thermal capacities and solution mass storage were assumed to be constant in this model. The solution and vapor mass flow rates were determined using the pressure differences between the vessels. Time step and heat transfer coefficients in the simulation were assumed to be constant. Sugano, et al. [2] developed a dynamic model for the absorption chiller driven by hot water and this model was used for controlling the system in part load applications. Cai, et al. [3] studied the transient behavior of a single-effect absorption chiller using ionic liquids. Several relations were used to predict the thermodynamic properties of ammonia-water solution causing the results to be erroneous. Furthermore, the concentrations of solution at the exit of the absorber as well as the generator were assumed to be equal to the concentration inside the absorber and generator, respectively. Kohlenbach and Ziegler [4] developed a dynamic model for a small single-effect absorption chiller on the basis of external and internal steady-state enthalpy balances. The results obtained from the simulation were compared with the experimental data. Zinet, et al. [5] developed a dynamic model for the simulation of a single-effect LiBr-H$_2$O absorption chiller. The machine was driven by two distinct heat sources. In contrast to previous works, the focus was on the detailed physical modeling of the heat and mass transfer phenomena occurring in the evaporator–absorber and in the desorber. The purpose of that approach was to reduce the dependence of the model on empirical and global parameters. An absorption chiller model used in an existing solar cooling system was developed by Marc, et al. [6] and presented the solar cooling plant, the metrology, and the control strategy. Secondly, the experimental results were analyzed and the steady-state chiller model and also the identification method were developed. Afterwards, the simplex method was used to determine the design parameters of the machine. An improved control algorithm that was proven to have high control performance was presented by Seo et al. [7]. Improving control performance was an important area for more complicated systems, such as triple-effect chillers or solar hybrid chillers. It was concluded that level control performance could be improved to vary within a narrower band by adding an additional level switch. Thermodynamic modeling of a double-effect LiBr-H$_2$O absorption refrigeration cycle was accomplished by Iranmanesh and Mehrabian [8]. Conductance of all components was evaluated based on the approach temperatures assumed as input parameters. The effect of input data on the cycle performance and the exergetic efficiency were also investigated.

This study deals with the dynamic analysis of a single-effect absorption chiller by considering the effect of quality on the solution concentration. Dynamic approach can be applied for controlling purposes. The fourth order Range-Kutta method is selected to solve the simultaneous equations deduced from continuity, momentum, and energy balances. The results inferred from the dynamic analysis are compared with the data from the steady-state condition. Obtaining major parameters such as coefficient of performance, second law efficiency, etc. as a function of time are the other objectives of this research.

2. Formulation of the dynamic model

2.1 Governing equations

The schematic diagram of a single-effect LiBr-H$_2$O absorption chiller is illustrated in Fig. 1. Each main component is characterized by a single pressure, temperature, and concentration. Several assumptions are made to simplify the simulation:

- The amount of heat diffusion in the flow direction is negligible.
- Neither the generator releases any heat to the surroundings nor does the evaporator receive any heat from the surroundings.
- The refrigerant at the exit of the evaporator is assumed to be at the state of saturated vapor.
- The refrigerant at the exit of the generator is assumed to be at the state of superheated vapor.
- The concentration of solution leaving the generator and absorber is different from the concentration inside the generator and absorber respectively.
- The input work of the pump is negligible.
- There is no pressure loss in the pipes.
- The fluid temperature at the exit of each component is the same as the temperature inside that component.

The governing equations for the dynamic analysis are:

Mass continuity:
$$\frac{d(M_i)}{dt} = \dot{m}_{in} - \dot{m}_{out} \tag{1}$$

Continuity of LiBr and water species:
$$\frac{d}{dt}(M_A Z_A) = \dot{m}_6 X_4 - \dot{m}_1 X_1 \tag{2}$$

$$\frac{d}{dt}(M_G Z_G) = \dot{m}_3 X_1 - \dot{m}_4 X_4 \tag{3}$$
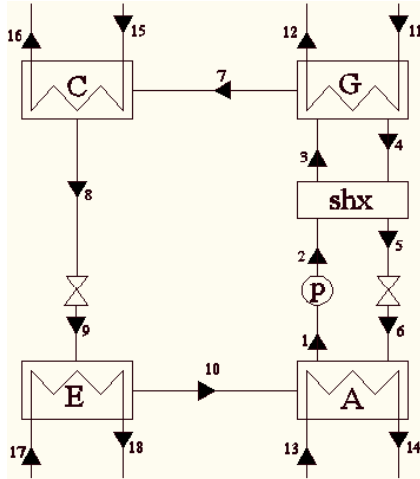
Fig. 1. Schematic diagram of a single-effect LiBr-H₂O absorption chiller

Momentum:

$$\frac{d\dot{m}_i}{dt} + \frac{1}{2}f_i\frac{\dot{m}_i|\dot{m}_i|}{\rho_i A_i D_i} = \frac{A_i}{L_i}(\Delta P) \qquad (4)$$

Energy balance:

$$\frac{d}{dt}(M_i h_i) = \dot{m}_{in}h_{in} - \dot{m}_{out}h_{out} \pm Q_i \qquad (5)$$

The concentration of solution at the exit of the absorber and generator is a function of the quality and solution concentration of generator and absorber respectively:

$$X_4 = \frac{Z_G}{(1-Qu_G)} \qquad (6)$$

$$X_1 = \frac{Z_A}{(1-Qu_A)} \qquad (7)$$

Now, Eqs. 2 and 3 lead to:

$$\frac{d}{dt}(M_A Z_A) = \dot{m}_6\frac{Z_G}{(1-Qu_G)} - \dot{m}_1\frac{Z_A}{(1-Qu_A)} \qquad (8)$$

$$\frac{d}{dt}(M_G Z_G) = \dot{m}_3\frac{Z_A}{(1-Qu_A)} - \dot{m}_4\frac{Z_G}{(1-Qu_G)} \qquad (9)$$

Z stands for the concentration of solution at the generator and absorber. X is the concentration of solution at the exit of the absorber and generator. As the quality approaches zero, the amount of Z will become equal to X. The following equations can be applied for the expansion valves and the pump:

$$\frac{1}{2}\xi\frac{1}{\rho_i A_V^2}\dot{m}_i|\dot{m}_i| = P_V^{in} - P_V^{out} \qquad (10)$$

$$\Delta P = a_0 + a_1\dot{m}_i + a_2\dot{m}_i^2 \qquad (11)$$

where ξ is the expansion valve friction factor which is assumed to be constant. A_V is the smallest cross-sectional area of the expansion valve. a_0, a_1, and a_2 can be obtained from the characteristic curve of the pump. To solve the simultaneous differential equations, a trial and error process is needed to calculate the pressure, temperature, and quality of the main components. In the second stage, the properties at other state points of the cycle can be obtained from the initial conditions. These amounts are used to solve the simultaneous differential equations and the amounts of parameters at the next step can be calculated. This process is repeated until the convergence criterion is satisfied.

The exergetic efficiency represents the reversible performance of the cycle and is defined as the ratio of total exergy taken from the system to the total exergy given to the system [9]:

$$\eta = \frac{\Delta E_{taken}}{\Delta E_{given}} = 1 - \frac{\sum \Delta E_{loss}}{\sum \Delta E_{given}} \qquad (12)$$

Table 1. Typical set of input data used in the dynamic analysis (Ref. [10])

C_{shx}	UA_A (kW.K⁻¹)	UA_C (kW.K⁻¹)	UA_E (kW.K⁻¹)	UA_G (kW.K⁻¹)	$\dot{m}_{11}$ (kg.s⁻¹)	T_{11} (°C)	$\dot{m}_{13}$ (kg.s⁻¹)	T_{13} (°C)	$\dot{m}_{15}$ (kg.s⁻¹)	T_{15} (°C)	$\dot{m}_{17}$ (kg.s⁻¹)	T_{17} (°C)
0.64	1.8	1.2	2.25	1.00	1.00	100	0.28	25.0	0.28	25	0.4	10.0

Table 2. Typical set of initial values of the simultaneous differential equations

h_G (kJ.kg⁻¹)	h_A (kJ.kg⁻¹)	h_C (kJ.kg⁻¹)	h_E (kJ.kg⁻¹)	M_G (kg)	M_A (kg)	M_C (kg)	M_E (kg)	Z_A (%LiBr)	Z_G (%LiBr)	$\dot{m}_7$ (kg.s⁻¹)	$\dot{m}_{10}$ (kg.s⁻¹)
1356.38	1384.58	1482.46	1249.93	15.06	15.72	2.54	2.36	27.33	32.32	0.00337	0.00448

Table 3. Comparison between the dynamic simulation results and steady-state ones (Ref. [10])

	Q_A (kW)	Q_G (kW)	Q_C (kW)	Q_E (kW)	COP	P_G (kPa)	P_A (kPa)	$\dot{m}_1$ (kg/s)	$\dot{m}_6$ (kg/s)	X_4 (%LiBr)	X_1 (%LiBr)
Ref. [10]	14.039	14.678	11.213	10.574	0.720	7.347	0.679	0.0500	0.0455	62.4	56.7
Current study	13.7927	14.7725	11.2327	10.5854	0.7166	7.35	0.67	0.0501	0.0454	62.2301	56.8234
Absolute value of relative error (%)	1.754	0.644	0.176	0.108	0.472	0.041	1.325	0.2	0.219	0.272	0.217

Table 4. Thermodynamic properties of state points corresponding to input data (Ref. [10])						
	$h(kJ.kg^{-1})$	$\dot{m}(kg.s^{-1})$	$P(kPa)$	$Qu(fraction)$	$T(^\circ C)$	$X\ (\%\ LiBr)$
1	85.8	0.0500	0.679	0.000	32.9	56.7
2	85.8	0.0500	7.347	-	32.9	56.7
3	147.0	0.0500	7.347	-	63.2	56.7
4	221.2	0.0455	7.347	0.000	89.4	62.4
5	153.9	0.0455	7.347	-	53.3	62.4
6	153.9	0.0455	0.679	0.006	44.7	62.4
7	2644.6	0.0045	7.347	-	76.8	0.0
8	167.2	0.0045	7.347	0.000	39.9	0.0
9	167.2	0.0045	0.679	0.064	1.5	0.0
10	2503.4	0.0045	0.679	1.000	1.5	0.0
11	418.9	1.0000	-	-	100.0	-
12	404.2	-	-	-	96.5	-
13	104.8	0.2800	-	-	25.0	-
14	154.9	-	-	-	37.0	-
15	104.8	0.2800	-	-	25.0	-
16	144.8	-	-	-	34.6	-
17	42.0	0.4000	-	-	10.0	-
18	15.6	-	-	-	3.7	-
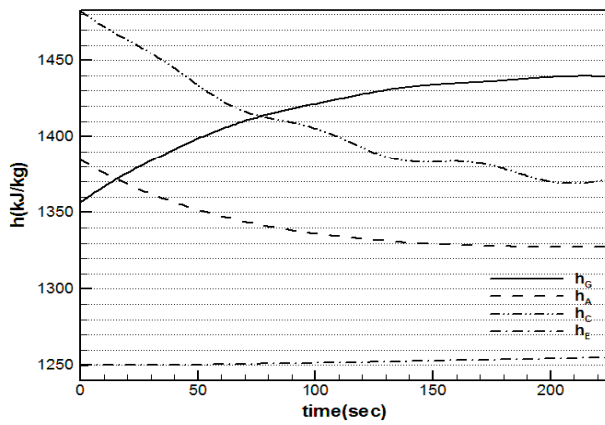
Fig. 2. Variation of the enthalpy of components versus time
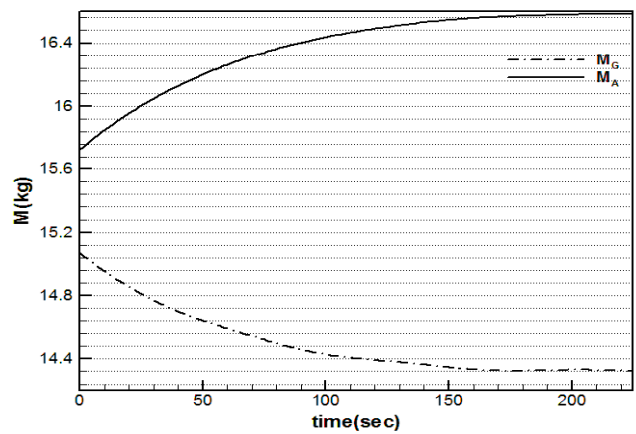
Fig. 3. Variation of the mass of solution in the generator and absorber versus time
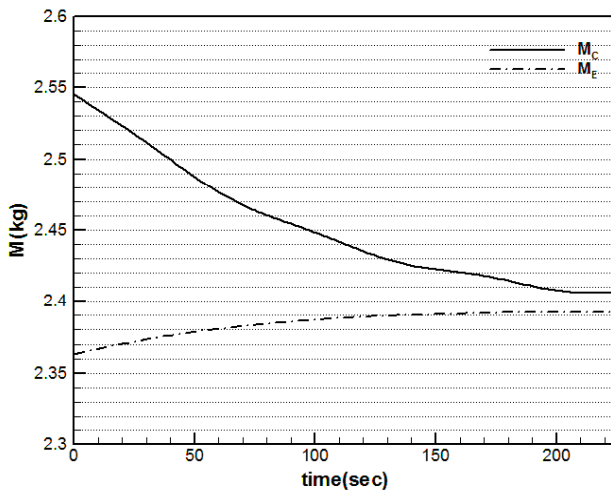
Fig. 4. Variation of the mass of refrigerant in the condenser and evaporator versus time
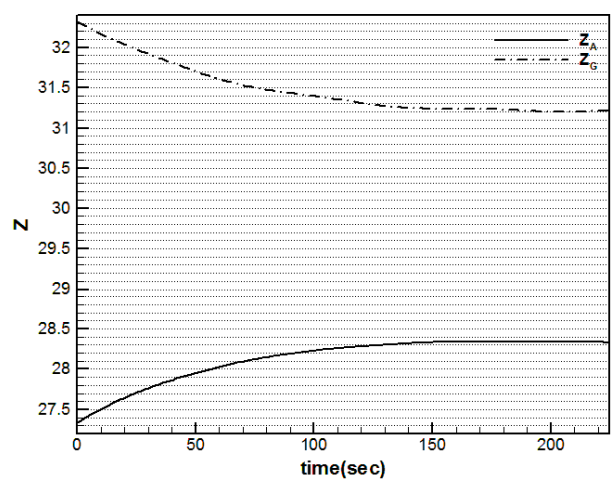
Fig. 5. Variation of the concentration of solution in the absorber and generator versus time
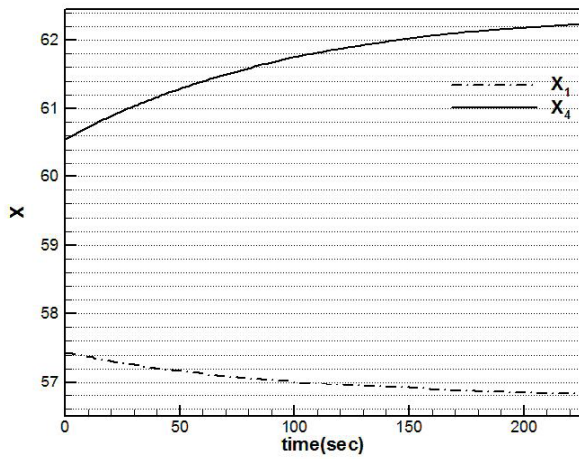
Fig. 6. Variation of the concentration of the solution at the exit of the absorber and generator versus time
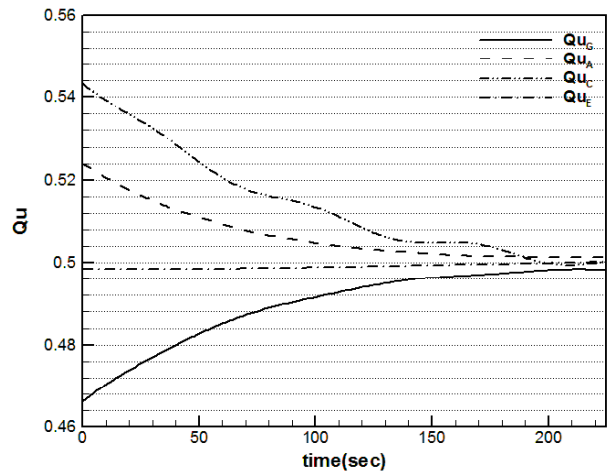
Fig. 7. Variation of the quality of components in the absorption system versus time
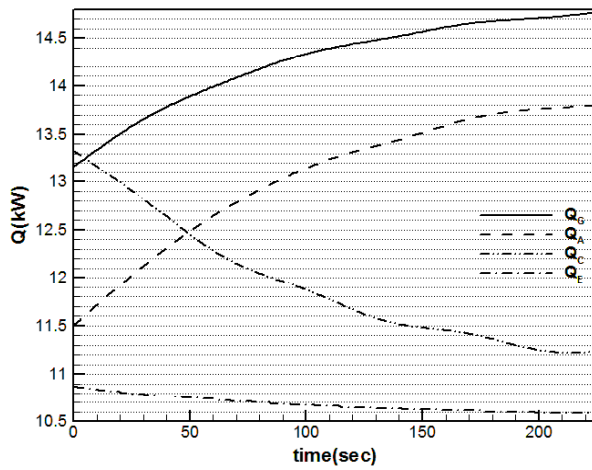
Fig. 8. Variation of the heat transfer rate of the components versus time
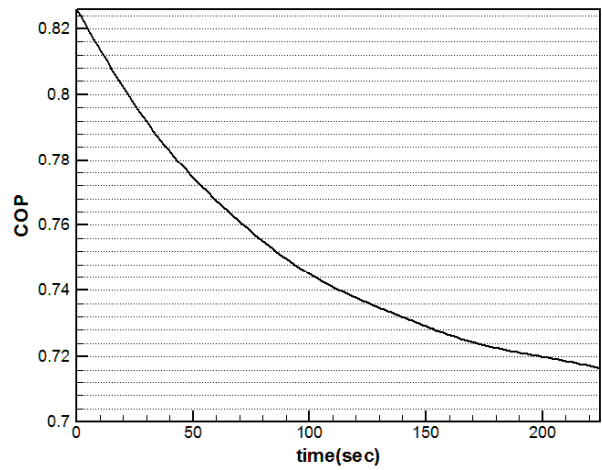
Fig. 9. Variation of the coefficient of performance of the cycle versus time
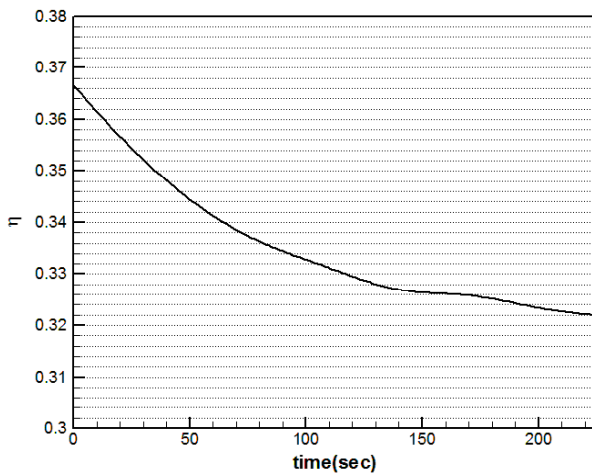
Fig. 10. Variation of the exergetic efficiency of the cycle versus time
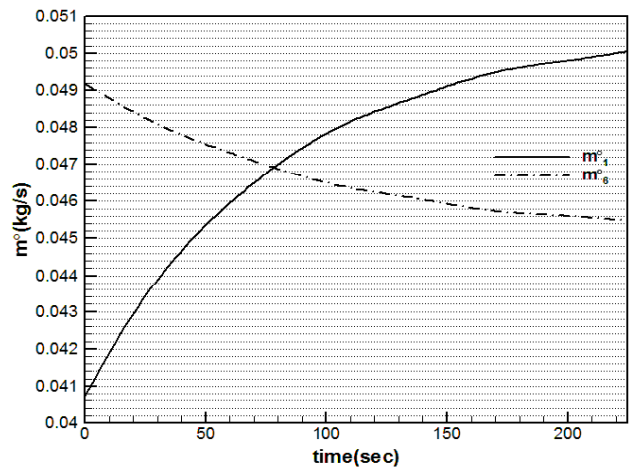
Fig. 11. Variation of the mass flow rate of solution at the exit of the generator and absorber versus time
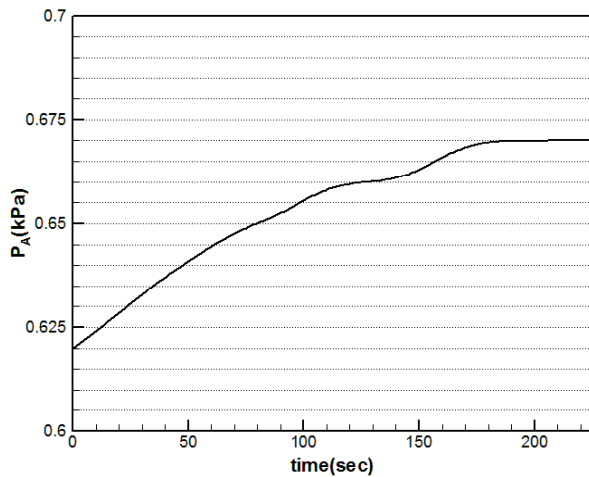
**Fig. 12. Variation of the absorber pressure versus time**
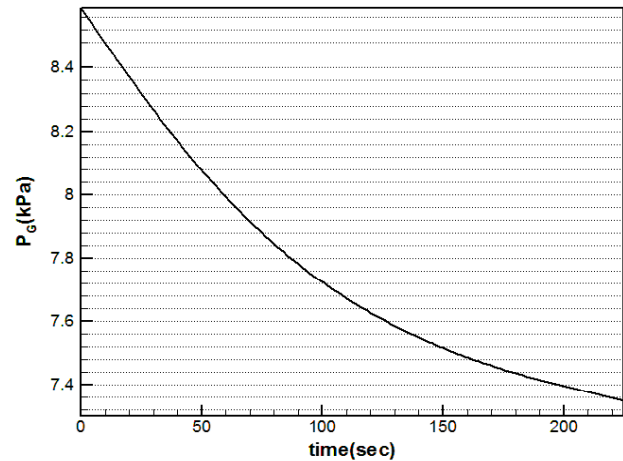
Fig. 13. Variation of the generator pressure versus time
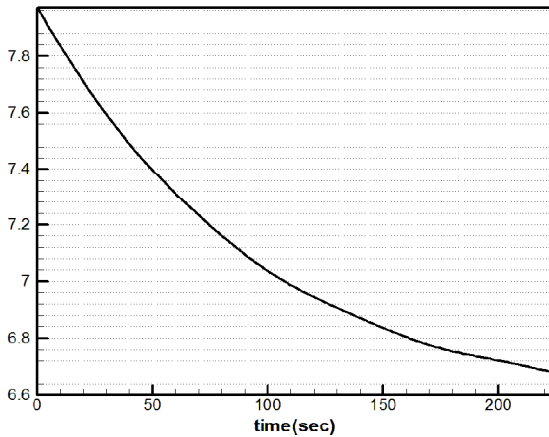
Fig. 14. Variation of the pressure difference between the generator and absorber versus time
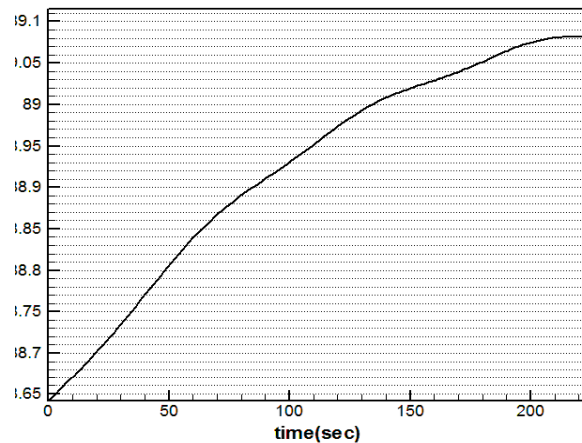
Fig. 15. Variation of generator temperature versus time

3. Results and discussion

The input data of the dynamic analysis is presented in Tables 1 and 2. Table 3 shows the comparison between dynamic analysis results and steady-state ones while thermodynamic properties of the state points corresponding to input data are represented in Table 4 (Ref. [10]). Transient behavior of different parameters namely enthalpy of main components, coefficient performance of the cycle, pressure difference between the generator and absorber etc. is illustrated in Figs. 2 to 15. Several initial conditions were used to complete the dynamic simulation of a single-effect absorption chiller. At the beginning of the simulation, the pressure difference between the generator and absorber is higher than the steady-state condition (Figs. 12 and 13). The mass flow rate at point 1 increases as the pressure difference between the generator and absorber is decreased according to the characteristic curve of the pump (Figs. 11 and 14). Conversely, the mass flow rate at point 6 decreases according to Eq. 10. It is very

interesting that in spite of increasing the amount of $\dot{m}_1$ and decreasing $\dot{m}_6$ (Fig. 11), an increase in M_A is observed while M_G decreases (Fig. 3). Although $\dot{m}_1$ is increasing, its rate is still lower than $\dot{m}_6$, leading to an increase in M_A and a decrease in M_G. $\dot{m}_7$ and $\dot{m}_{10}$ have a negligible effect on M_A and M_G, because they are smaller than $\dot{m}_1$ and $\dot{m}_6$. Although rich solution leaves the generator at the higher rate in comparison with weak solution, increasing Q_G leads to an increase in X_4 and Qu_G (Figs. 6, 7 and 8). Temperature of generator increases because of a decrease in pressure and an increase in X_4. This is in agreement with Duhring diagram [11]. At the absorber, rich solution absorbs the refrigerant vapor at a higher rate leading to a decrease in Qu_A and releasing more heat (Figs. 7 and 8). The coefficient of performance and the second law efficiency decrease because of an increase in Q_G and a decrease in Q_E (Figs. 8 and 9).

4. Verification

To run the computer code, several initial values were assumed (Table 2). The results obtained from the dynamic simulation were compared with the steady-state results since the input parameters were assumed to be the same as those in Ref. [10] (Table 1). However, the results show that dynamic analysis results are in agreement with the steady-state ones within utmost 2% relative error based on Table 3.

5. Conclusions

In This study a dynamic analysis of a single-effect absorption chiller by considering the effect of quality on concentration was conducted. Moreover, a transient analysis of exergy was achieved to determine the exergetic efficiency in terms of time. The simultaneous differential equations were solved using the fourth order Runge-Kutta method. To verify the model, the results inferred from the dynamic simulation were compared with those obtained in the steady-state approach. Furthermore, dynamic behavior of a single-effect absorption chiller was investigated analytically confirming the veracity of the developed model. Based on the deduced results, the coefficient of performance (COP) and exergetic efficiency will both decrease and finally approach the steady-state values. However, the results are in good agreement with the ones derived from the steady-state analysis. Additionally, as the quality approaches zero, the effect of concentration can be neglected. Dynamic analysis can be applied for control purposes to maximize the coefficient of performance.

Nomenclature

a_0, a_1, a_2	Pump characteristics
A	Pipe cross sectional area
A_V	The smallest cross-sectional area of the expansion valve, m^2
COP	Coefficient of performance
D	Pipe diameter, m
E	Exergy, kJ
f	The pipe friction factor
h	Enthalpy, $Kj.kg^{-1}$
L	Pipe length, m
M	The mass in each component, kg
$\dot{m}$	Mass flow rate, $kg.s^{-1}$
P	Pressure, kPa
Q	Heat transfer rate, kW
Qu	Quality
T	Temperature, $^{\circ}C$
t	Time, sec
UA	Conductance, $kW.K^{-1}$
X	Concentration of solation at the exit of generator and absorber
Z	Concentration of solution at the absorber and generator

Greek symbols

ξ	The expansion valve friction factor
ρ	Density, kg/m^3
η	Exergetic efficiency
ε	Heat exchanger effectiveness
Δ	Difference

Subscripts

A	Absorber
C	Condenser
E	Evaporator
G	Generator
i	Number of state points
in	Inlet
P	Pump
out	Outlet
shx	Solution heat exchanger
V	Expansion valve

References

[1] Jeong, S., Kang, B.H., and Karng, S.W., "*Dynamic simulation of an absorption heat pump for recovering low grade waste heat*", Applied Thermal Engineering, Vol. 18, pp. 1-12, 1998.

[2] Sugano, N., Saito, K., Kawai, S., Nisiyama, N., Honma, R., and Wakimizu, H., "*Simulation and experimental research of dynamic characteristics of single-effect absorption refrigerators driven by waste hot water*", Trans. JSME, Vol. 60, pp. 290-296, 1994.

[3] Cai, W. Sen, M., and Paolucci, S., "*Dynamic modeling of an absorption refrigeration system using ionic liquids*", ASME International Mechanical Engineering Congress and Exposition, Seattle, Washington, USA, pp. 1-9, 2007.

[4] Kohlenbach, P., and Ziegler, F., "*A dynamic simulation model for transient absorption chiller performance*", International Journal of Refrigeration, Vol. 31, pp. 217-225, 2008.

[5] Zinet, M., Rulliere, R., and Haberschill, P., "*A numerical model for the dynamic simulation of a recirculation single-effect absorption chiller*", Energy Conversion and Management, Vol. 62, pp. 51–63, 2012.

[6] Marc, O., Anies, G., Lucas, F., and Castaing-Lasvignottes, J., "*Assessing performance and controlling operating conditions of a solar driven absorption chiller using simplified numerical models*", Solar Energy, Vol. 86, pp. 2231–2239, 2012.

[7] Seo, J., Shin, Y., and Dong Chung, J., "*Dynamics and control of solution levels in a high temperature generator for an absorption chiller*", International Journal of Refrigeration, Vol. 35, pp. 1123-1129, 2012.

[8] Iranmanesh, A., and Mehrabian, M.A. "*Thermodynamic modeling of a double-effect LiBr-H2O absorption refrigeration cycle*", Heat and Mass Transfer, Vol. 48, pp. 2113-2123, 2012.

[9] Mehrabian, M. A., and Shahbeik, A.E., "*Thermodynamic modeling of a single-effect LiBr-H2O absorption refrigeration cycle*", Proc. IMechE Part E, Vol. 219, pp. 261-273, 2004.

[10]   Herold, K.E., Radermacher, R., and Klein, S.A. *"Absorption chillers and heat pumps"*, CRC Press Inc., Boca Raton, New York, London, Tokyo, 1996.

[11]   Lee, H.R., Koo, K.K., Jeong, S., Kim, J.S., Lee, H., Oh, Y.S., Park, D.R., and Baek, Y.S., *"Thermodynamic design data and performance evaluation of the water + lithium bromide + lithium iodide + lithium nitrate + lithium chloride system for absorption chiller"*, Applied Thermal Engineering, Vol. 20, pp. 707-720, 2000.